Journal of Chromatography A, 1395 (2015) 152–159

Contents lists available at ScienceDirect

Journal of Chromatography A

journal homepage: www.elsevier.com/locate/chroma

Non-targeted analysis of electronics waste by comprehensive two-dimensional gas chromatography combined with high-resolution mass spectrometry: Using accurate mass information and mass defect analysis to explore the data

Masaaki Ubukata[a], Karl J. Jobst[b], Eric J. Reiner[b], Stephen E. Reichenbach[c], Qingping Tao[d], Jiliang Hang[d], Zhanpin Wu[e], A. John Dane[a], Robert B. Cody[a,*]

[a] JEOL USA, Inc., Peabody, MA, USA
[b] Ontario Ministry of the Environment and Climate Change, Etobicoke, ON, Canada
[c] University of Nebraska-Lincoln, Lincoln, NE, USA
[d] GC Image LLC, Lincoln, NE, USA
[e] Zoex Corporation, Houston, TX, USA

ARTICLE INFO

Article history:
Received 18 December 2014
Received in revised form 18 March 2015
Accepted 22 March 2015
Available online 28 March 2015

Keywords:
Two-dimensional gas chromatography
Kendrick mass defect
Mass spectrometry
Environmental
Time-of-flight
GC×GC–HRMS

ABSTRACT

Comprehensive two-dimensional gas chromatography (GC×GC) and high-resolution mass spectrometry (HRMS) offer the best possible separation of their respective techniques. Recent commercialization of combined GC×GC–HRMS systems offers new possibilities for the analysis of complex mixtures. However, such experiments yield enormous data sets that require new informatics tools to facilitate the interpretation of the rich information content.

This study reports on the analysis of dust obtained from an electronics recycling facility by using GC×GC in combination with a new high-resolution time-of-flight (TOF) mass spectrometer. New software tools for (non-traditional) Kendrick mass defect analysis were developed in this research and greatly aided in the identification of compounds containing chlorine and bromine, elements that feature in most persistent organic pollutants (POPs). In essence, the mass defect plot serves as a visual aid from which halogenated compounds are recognizable on the basis of their mass defect and isotope patterns. Mass chromatograms were generated based on specific ions identified in the plots as well as region of the plot predominantly occupied by halogenated contaminants. Tentative identification was aided by database searches, complementary electron-capture negative ionization experiments and elemental composition determinations from the exact mass data. These included known and emerging flame retardants, such as polybrominated diphenyl ethers (PBDEs), hexabromobenzene, tetrabromo bisphenol A and tris (1-chloro-2-propyl) phosphate (TCPP), as well as other legacy contaminants such as polychlorinated biphenyls (PCBs) and polychlorinated terphenyls (PCTs).

1. Introduction

Comprehensive two-dimensional gas chromatography (GC×GC) [1] in combination with high-resolution mass spectrometry (HRMS) is a powerful tool for the analysis of complex mixtures [2–6]. Hundreds or even thousands of compounds can be separated and detected using this type of system. However, interpreting the data sets generated by a GC×GC/HRMS system can be challenging due to the large amount of information the data offers.

The traditional approach to identify chemical compounds in a mixture involves the careful interpretation of their (chromatographically-resolved) mass spectra [7], often with the aid of mass spectral libraries and comparison with genuine analytical standards. With GC×GC–MS, this time-consuming process can be simplified by filtering the enormous data sets, using automated software and scripting [8–10], and focusing on classes of compounds that share a common structure motif of interest. As a prime example, chlorine and bromine containing compounds display clearly recognizable isotope patterns in their mass spectra, and

* Corresponding author. Tel.: +1 978 536 2396.
E-mail address: cody@jeol.com (R.B. Cody).

http://dx.doi.org/10.1016/j.chroma.2015.03.050
0021-9673/

they may well account for the majority of known and emerging persistent organic pollutants (POPs) [11,12].

The mass resolution and exact mass information offered by high-resolution time-of-flight mass spectrometry (HR-TOFMS) can mitigate the effects of matrix interferences and significantly improve the confidence of target compound identification. These features also offer enhanced capabilities to identify unknown compounds, including POPs. Hashimoto et al. [4–6] have recently employed this technique to selectively identify organohalogen contaminants in environmental and biological samples. Their strategy hinges on the unique mass differences of 1.997 Da between the two principal stable isotopes of Cl and Br. Combining this information with the measured isotope ratios enables fast, automated visualization of the known and unknown POPs in the GC×GC chromatogram.

The challenge of interpreting high-resolution mass spectrometry data was recognized early on. In 1963, Kendrick [13] realized that by converting the International Union of Pure and Applied Chemistry (IUPAC) mass scale (C = 12.000 Da) to one in which CH_2 = 14.000 Da (Equation (1)), organic ions belonging to a homologous series have identical Kendrick mass defects (Equation (2)). Examples of Kendrick masses and Kendrick mass defects (KMD) for methyl, ethyl, and propyl naphthalene are listed in the supplementary data (Table S1). This approach greatly simplifies the high-resolution mass spectrometric data analysis because homologous compounds share the same KMD.

$$\text{Kendrick mass} = \text{IUPAC mass} \times \left(\frac{14}{14.01565}\right) \quad (1)$$

$$\text{Kendrick mass defect} = \text{nominal Kendrick mass} - \text{exact Kendrick mass} \quad (2)$$

HRMS data can also be represented graphically by constructing a Kendrick Mass Defect Plot [14], which has seen extensive use in the analysis and chemical fingerprinting of petroleum samples [15]. More recently, the Kendrick Mass Defect Plot has been proposed as a powerful tool for the identification of POPs by HRMS. The use of non-traditional mass scales, such as −H/+Cl (34/33.96102), −H/+Br (78/77.91051) [16–18], CF_2 (50/49.99681), and +F/−Cl (16/15.97045) [19] substitutions, eases the identification of Br, Cl, and F containing compound in complex environmental samples. These plots can act as guide in the interpretation of highly complex GC×GC–HRTOF data sets: ions of interest may be identified by visual inspection of the plot and corresponding isomers can be investigated in the (GC×GC) chromatographic space [18].

To date, little work combining GC×GC and mass defect analysis has been done. In this study, we analyzed a dust sample collected from an electronics recycling facility by using a GC×GC in combination with a new high-resolution time-of-flight (TOF) mass spectrometer. We specifically chose dust as the sample matrix because it reflects current exposure of humans to POPs [20,21] and, as noted by Hilton et al. [8], dust is a complex matrix that requires a powerful separation technique, such as GC×GC. Nontraditional Kendrick mass defect plots using the substitution of a hydrogen with a chlorine atom were used to facilitate the identification of halogenated compounds in an electronic waste sample [2]. This was further aided by database search results combined with elemental composition determinations from exact-mass data. In this work, new software methods and tools were developed (and incorporated into commercially available software) to construct KMD plots for selected regions of GC×GC chromatograms, to select ions of interest in those plots, and to generate selected ion chromatograms for visualization and analysis.

2. Experimental

2.1. Sample preparation

The dust sample was collected from the floor sweepings of an electronics recycling facility in Canada. No further sieving or separation was performed. Extraction of 1 g of dust sample was performed by ultrasonication in hexane (3 × 15 mL). Each 15 mL aliquot was ultrasonicated for 10 min, then decanted and the volumes were combined. The extract (45 mL final volume) was centrifuged using an Eppendorf Centrifuge Model 5810 at 10,000 rpm for 10 min. The supernatant was dried with sodium sulfate (3 g packed a Pasteur pipette) and analyzed by GC×GC/HR-TOFMS.

2.2. Instrument conditions and data analysis

2.2.1. GC×GC/HR-TOFMS system

Sample measurements were carried out using a 7890A GC (Agilent Technologies, Santa Clara, CA, USA) with a ZX2 thermal modulator (Zoex, Houston, TX, USA) in combination with a JMS-T100GCV 4G (JEOL, Tokyo, Japan) HR-TOFMS system with a resolving power specification of 8000 (FWHM definition) and a mass accuracy specification of 5 ppm or 0.002 u. In this study, we performed GC×GC measurements using both electron ionization (EI) mode and electron-capture negative-ion (ECNI) mode. The instrument parameters are listed in Table 1.

2.2.2. Mass calibration

A single-point external mass drift compensation was performed for the whole mass calibration following data acquisition by

Table 1
GC×GC/HR-TOFMS conditions for dust sample measurement.

GC×GC	
GC	Agilent 7890A
GC×GC thermal modulator	Zoex ZX2
1st column	Rxi-5SilMS, 30 m length, 0.25 mm I.D., 0.25 μm film thickness
2nd column	Rxi-17SilMS, 2 m length, 0.15 mm I.D., 0.15 μm film thickness
Column connections	Glass press-fit unions sealed with polyimide glue
Modulation loop	Deactivated fused silica, 1.5 m, 0.15 mm I.D.
Secondary oven	None. Both columns operate at the same temperature
Oven program	50 °C (1 min) → 5 °C/min → 320 °C (5 min), total: 60 min
Injector temperature	280 °C
Injection mode	Splitless, purge time = 1 min
Flow rate	2 mL/min, constant flow, helium
Initial head pressure	200 kPa at oven temperature 50 °C
Moduration period	8 s
Modulation duration	0.4 s
Modulator hot jet program	250 °C → 5 °C/min → 350 °C (40 min), total: 60 min
Modulator cold jet	−90 °C (closed cycle refrigerator)
HR-TOFMS	
TOFMS	JEOL JMS-T100GCV 4G
Ionization mode	EI: 70 eV, 300 μA ECNI: 150 eV, 300 μA, ammonia/methane mix gas 0.5 mL/min
m/z range	EI: 45–800 ECNI: 30–800
Ion source temperature	EI: 250 °C ECNI: 200 °C
MS transfer line temperature	280 °C
Acquisition time	0.02 s (50 Hz)

using one column bleed peak corresponding to $C_5H_{15}O_3Si_3^+$, m/z 207.0329, in EI mode, and one background peak corresponding to ReO_3^-, m/z 234.9405, in ECNI mode.

2.2.3. Nontraditional KMD plot

An average mass spectrum for the entire retention time region was created by summing the mass spectra for all data points in GC×GC/HR-TOFMS data sets. Nontraditional KMD plots were created by converting the measured IUPAC m/z to −H/+Cl mass scales corresponding to the mass of a chlorine atom minus the mass of a hydrogen atom. The nominal mass was plotted versus the corresponding mass defect for each peak.

$$-\mathrm{H}/+\mathrm{Cl\,mass} = \mathrm{IUPAC\,mass} \times \left(\frac{34.0}{33.96102}\right) \quad (3)$$

$$\mathrm{H}/+\mathrm{Cl\,mass\,defect} = \mathrm{nominal} - \mathrm{H}/+\mathrm{Cl\ mass} - \mathrm{exact} - \mathrm{H}/+\mathrm{Cl\,mass} \quad (4)$$

Mass defect plots facilitated rapid identification of families of compounds that differ by the number of chlorine substituents. The KMD plots for −H/+Cl and −H/+Br are nearly identical, allowing us to view both Cl and Br substitutions in one plot.

2.2.4. Data processing

JEOL Mass Center software was used for data acquisition and to create a composite spectrum. GC Image® R2.5 Software (GC Image, LLC, Lincoln, NE, USA) with support for high-resolution data was used to view and process the GC×GC data and for database searching and elemental composition determinations. As detailed in the next section, new software methods and tools were developed within the GC Image software in collaboration with the Ontario Ministry of the Environment and used to identify families of halogenated contaminants.

3. Results and discussion

3.1. GC×GC/HR-EI measurement result

Fig. 1 shows the two-dimensional (2D)-EI total ion current (TIC) chromatogram for an electronic waste sample. The two columns separate components by different physical properties, providing a more complete separation than could be achieved by using a single column. In Fig. 1, the x-axis represents the retention time on Column 1, which in this case separates compounds by boiling point. The y-axis represents the retention time on Column 2, which separates components by polarity. Each spot (or "blob" in GC Image terminology) on the 2D chromatogram represents an eluting component. The spot colors represent abundance, and each spot on the 2D chromatogram consists of a set of mass spectra for that eluting compound. Different compound classes occupy different regions on the 2D chromatogram.

The large number of peaks observed in Fig. 1 easily surpasses what could be achieved using traditional capillary GC, but the interpretation remains a challenge. This is because the identification of a compound on the basis of their mass spectrum is not trivial, even with the aid of mass spectral libraries. This problem is exacerbated by the sheer number of compounds resolved in a single GC×GC experiment. Furthermore, the overlapping groups of peaks displayed in Fig. 1 obscure the ordered patterns that are helpful in identifying structurally related compounds. Improving the separation (e.g. through modification of the column chemistry) is unlikely to resolve these issues, especially in the case of a complex mixture. Alternatively, the accurate mass information obtained from a high-resolution TOF mass spectrometer can be used to explore the data.

An average mass spectrum for the entire retention time region is shown in Fig. 2a. The average mass spectrum (computed by summing all spectra, as described in Section 3.3) displays a large number of the peaks in the low m/z region, as well as an intense GC column bleed peak corresponding to $C_5H_{15}O_3Si_3^+$, m/z 207.0329. While some specific halogen isotope patterns (m/z 551.518 e.g.) are observed in the higher m/z region (see inset of Fig. 2a), a more convenient way to identify halogenated compounds in the mass spectrum is to construct a non-traditional Kendrick mass defect plot. The exact mass for each ion was converted to the −H/+Cl mass scale (Equation (3)). An −H/+Cl mass defect plot for the average mass spectrum was constructed as shown in Fig. 2b, by graphing the exact −H/+Cl mass versus the corresponding −H/+Cl mass defect for each mass spectral peak.

Fig. 2(b) shows that ions in each class of halogenated compounds differing by −H/+Cl substitution align with the horizontal axis because they have the same −H/+Cl mass defect. This is also true for compounds that differ by −H/+Br substitution because the scaling factor for −H/+Cl (34/33.96102) and −H/+Br (78/77.91051) substitutions are very close. In addition, one can visually recognize halogenated compounds on the basis of the unique isotope pattern of polychlorinated and polybrominated compounds. The

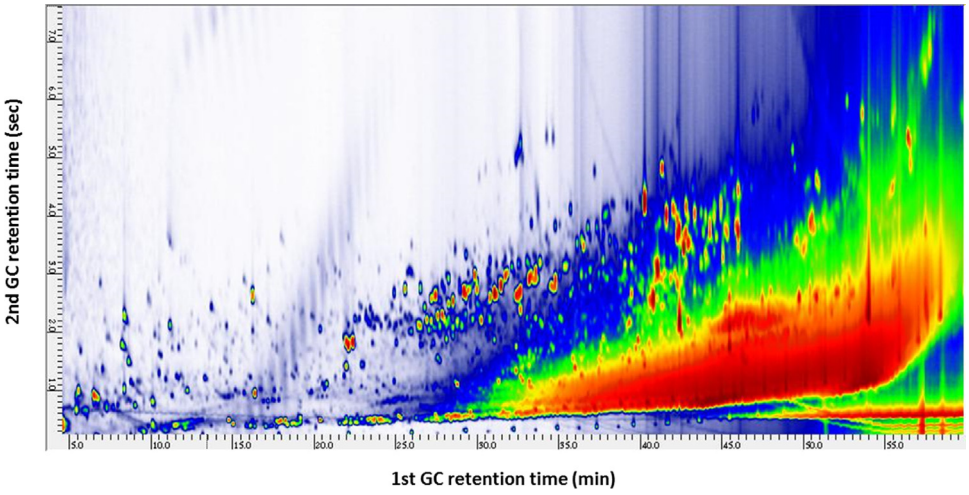

Fig. 1. 2D-EI total ion current chromatogram of a dust sample.

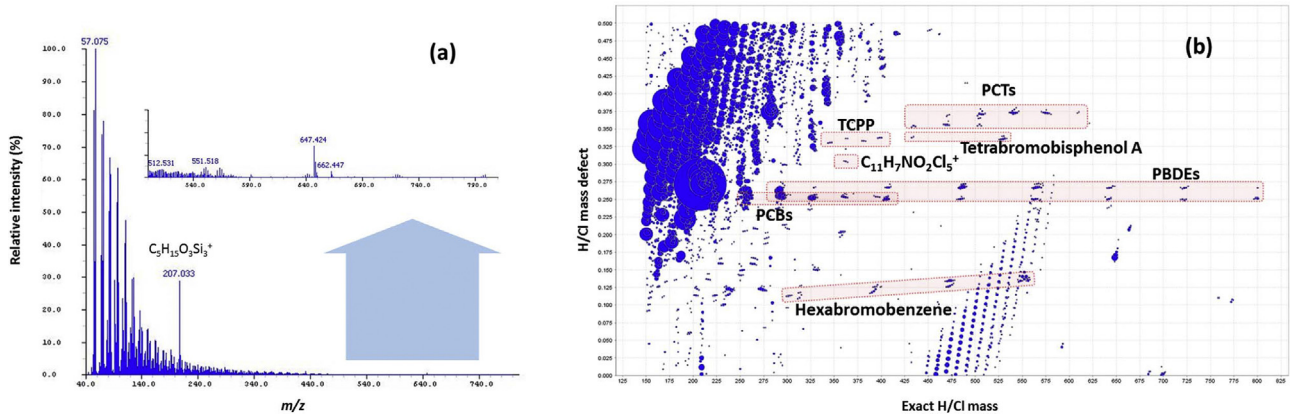

Fig. 2. (a) Averaged EI mass spectrum for the entire retention time region, (b) the −H/+Cl mass defect plot for the averaged EI mass spectrum.

exact mass measurement afforded by the HRTOFMS, in combination with a molecular formula calculator, can yield tentative identification of the compounds or compound classes. The accurate mass measurement results are listed in Table 2. All measured ions had good mass accuracy: less than 1 mDa mass error using the column bleed peak corresponding to $C_5H_{15}O_3Si_3^+$ (m/z 207.0329) as the single-point external mass drift compensation. NIST library database searches were also used to confirm the identifications. This approach led to the identification of Tris (1-chloro-2-propyl) phosphate (TCPP), Polychlorinated terphenyls (PCTs), Polychlorinated biphenyls (PCBs), Tetrabromobisphenol A, Polybrominated diphenyl ethers (PBDEs), and Hexabromobenzene.

Most compounds produced a match factor over 800 using NIST library database search. A perfect match is designated by a match factor of 999 with match factors above 800 generally being considered reasonable matches. However, the mass spectra of several compounds, including Octachlorobiphenyl, Dibromodiphenyl ether, and Heptabromodiphenyl ether, displayed significant interference from the dust matrix, resulting in match factors around 700. The quality of mass spectral matches would be much poorer had GC×GC separation not been employed. In these cases, the accurate mass measurements allowed for confident molecular formula determination. The accurate mass measurements of the HR-TOFMS system can significantly enhance NIST library database searches for chemical identification and to confirm their elemental compositions. Ultimately, comparison with genuine analytical standards is necessary to confirm the tentative identifications provided by the above approach.

The mass defect plot of Fig. 2b greatly simplified the identification of halogenated compounds in the complex 2D chromatogram. Using new software methods and tools developed in this work (and described in Section 3.3), selected ion chromatograms (SICs) can be generated automatically by simply drawing a polygon around the ions of each class of halogenated compounds. Fig. 3 shows the high-resolution 2D SICs for the most abundant isotope molecular ions selected in this way for each class of halogenated compounds. Note that the ±50 ppm value is 10 times greater than the mass accuracy of the mass spectrometer. This is not a limitation of the software, or

Table 2
2D-EI accurate mass measurement and NIST library database search results.

Compound	The number of halogens	Most abundant isotope molecular ion				NIST library search result	
		Elemental composition	Theoretical m/z	Measured m/z	Mass error (mDa)	Match factor	R. Match factor
Tris (1-chloro-2-propyl) phosphate (TCPP)	Cl: 5	$C_8H_{13}Cl_5O_4P$	380.8965	380.8964	−0.1	865	899
Polychlorinated terphenyls (PCTs)	Cl: 8	$C_{18}H_6Cl_8$	505.7920	505.7913	−0.7	n/a	n/a
	Cl: 9	$C_{18}H_5Cl_9$	539.7530	539.7527	−0.3	n/a	n/a
	Cl: 10	$C_{18}H_4Cl_{10}$	573.7141	573.7147	0.6	n/a	n/a
	Cl: 11	$C_{18}H_3Cl_{11}$	607.6751	607.6751	0.0	n/a	n/a
Polychlorinated biphenyls (PCBs)	Cl: 4	$C_{12}H_6Cl_4$	291.9195	291.9190	−0.5	837	870
	Cl: 5	$C_{12}H_5Cl_5$	325.8805	325.8796	−0.9	875	914
	Cl: 6	$C_{12}H_4Cl_6$	359.8415	359.8409	−0.6	841	913
	Cl: 7	$C_{12}H_3Cl_7$	393.8025	393.8024	−0.1	870	912
	Cl: 8	$C_{12}H_2Cl_8$	429.7606	429.7601	−0.5	679	809
1,3,4,6,7,7-hexachloro-N-ethyl-bicyclo [2,2,1]hept-5-en-2,3-dicarboximide	Cl: 6	$C_{11}H_7NO_2Cl_5(M–Cl^+)$	361.8891	361.8887	−0.4	823	841
Tetrabromobisphenol A	Br: 4	$C_{14}H_9Br_4O_2$	528.7296	528.7289	−0.7	873	875
Polybrominated diphenyl ethers (PBDEs)	Br: 2	$C_{12}H_8Br_2O$	327.8922	327.8915	−0.7	677	876
	Br: 3	$C_{12}H_7Br_3O$	405.8027	405.8020	−0.7	890	903
	Br: 4	$C_{12}H_6Br_4O$	485.7112	485.7114	0.2	836	881
	Br: 5	$C_{12}H_5Br_5O$	563.6217	563.6208	−0.9	881	900
	Br: 6	$C_{12}H_4Br_6O$	643.5302	643.5299	−0.3	832	853
	Br: 7	$C_{12}H_3Br_7O$	721.4407	721.4399	−0.8	694	697
Hexabromobenzene	Br: 6	C_6Br_6	551.5039	551.5041	0.2	826	834

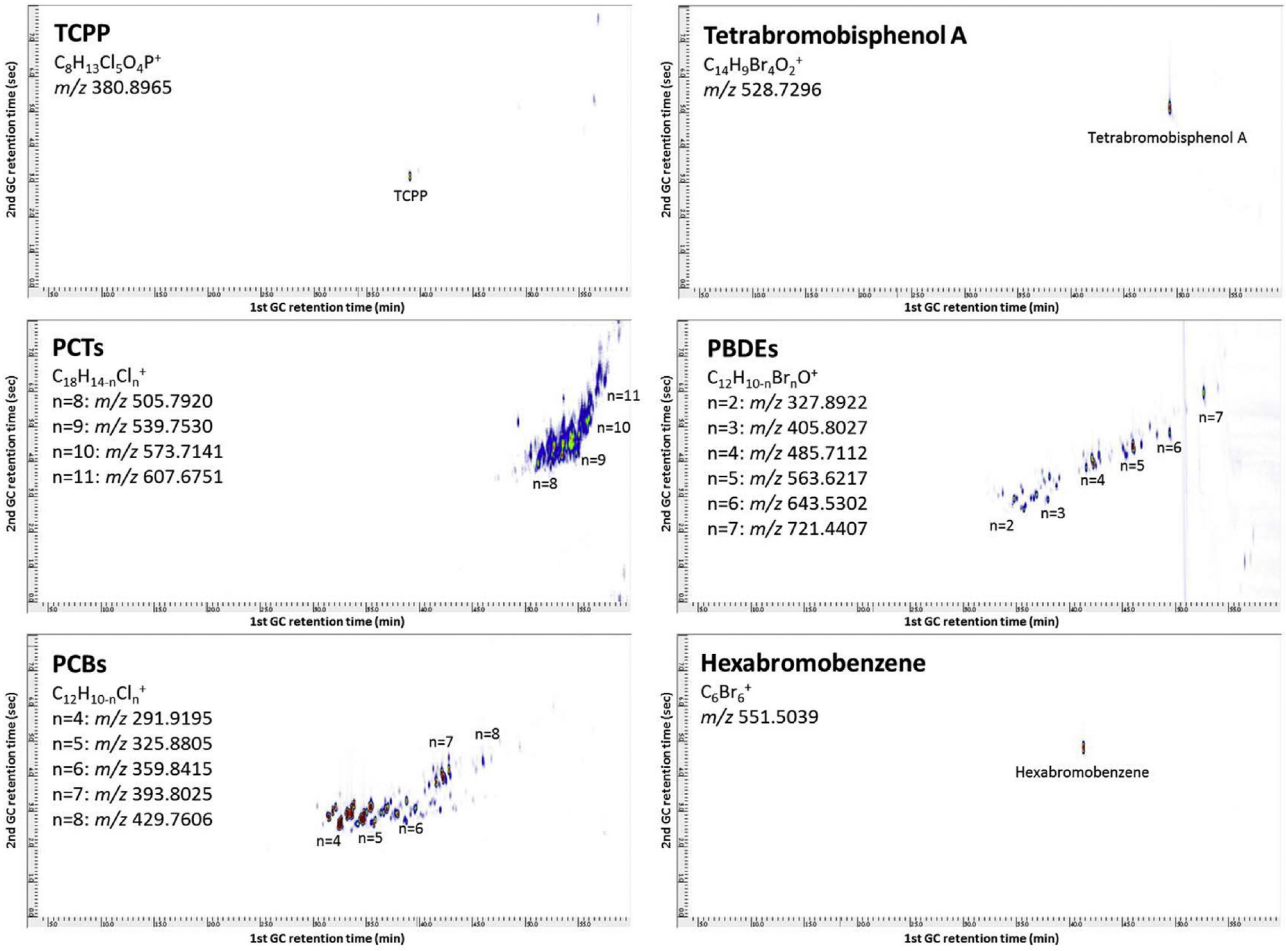

Fig. 3. 2D-EI extracted ion chromatograms for theoretical *m/z* of the most abundant isotope molecular ions ±50 ppm.

of the mass spectrometer. The 50 ppm value was chosen to reflect the peak width of the profile (raw data) mass spectral peaks in the uncentroided data set that was used to create the SIC's. Alternatively, the SIC's could be created from centroided data, which would permit a narrower mass tolerance such as ±5 ppm.

This approach also paves the way for discovery of new or unexpected polyhalogenated compounds. For example, the cluster of ions with the assigned elemental composition $C_{11}H_7NO_2Cl_5^+$ is easy to spot in Fig. 2b. The corresponding SIC (not shown) displays a single peak, whose mass spectrum is virtually identical with the NIST entry for 1,4,5,6,7,7-hexachloro-N-ethyl-bicyclo [2,2,1]hept-5-en-2,3-dicarboximide, as shown in Fig. 4. The $C_{11}H_7NO_2Cl_5^+$ peak observed in Fig. 2b is actually the M–Cl ion. The compound yields a weak molecular ion under EI conditions. The origin and purpose of this chemical compound is not yet known. However, its structure is akin to the Dechlorane family of flame retardants [22] and, considering the sample is a composite of dust from a consumer electronics recycling facility, it may well be widely distributed.

3.2. GC×GC/HR-ECNI measurement result

Supplementary Fig. S5a shows the 2D-ECNI TIC chromatogram for the electronics waste sample. The ECNI technique is a lower-energy process than EI and can be used for the analysis of compounds containing electronegative elements such as halogens. In the 2D-ECNI TIC chromatogram, the dust sample matrix was reduced significantly compared with the 2D-EI TIC chromatogram.

On the other hand, some compounds showed abundant Cl^- and Br^- peaks instead of molecular ions. The ECNI method is especially good for low-concentration samples and quantitative analysis. Fig. S5b shows the high-resolution 2D-ECNI SICs for the selected isotope molecular ions for chlorine and bromine.

An average mass spectrum for the entire retention time region is shown in Supplementary Fig. S6a. Some halogenated compounds are recognizable in the −H/+Cl mass defect plot for the average ECNI

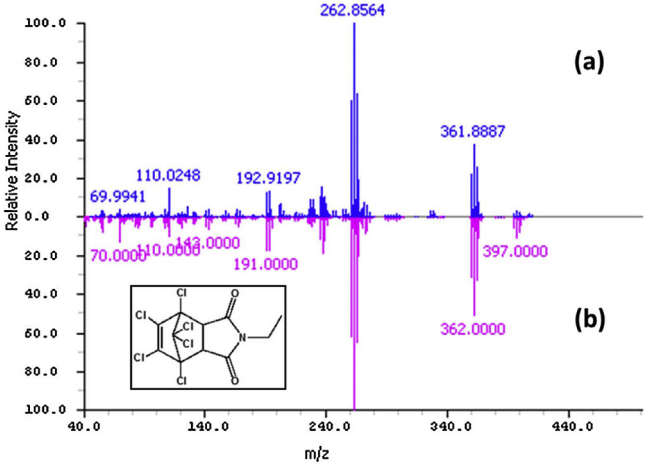

Fig. 4. EI mass spectra of 1,4,5,6,7,7-hexachloro-N-ethyl-bicyclo [2,2,1]hept-5-en-2,3-dicarboximide (a) measured, (b) NIST database.

mass spectrum shown in Fig. S6b. The mass defect plot obtained from the ECNI experiment (Fig. S6b) is similar to the EI data (Fig. 2b). In some cases, the ECNI technique enhanced the yield of molecular ions.

The ECNI chlorine mass chromatogram looks similar to the merged EI mass chromatograms for PCTs and PCBs. Also, the ECNI bromine mass chromatogram looks similar to the EI mass chromatograms for PBDEs.

3.3. Software development for GC×GC mass defect analysis

The combination of GC×GC and accurate-mass HRMS offers new opportunities for mass-defect analysis. In particular:

- A selected subregion of the GC×GC retention-times plane can be used to specify a subset of spectra for mass-defect analysis. GC×GC provides excellent selectivity and resolution as well as two-dimensional patterns related to chemical structure. These attributes of 2D separations facilitate the selection of compound groups of interest in the 2D retention-times plane while excluding other compounds and/or undesirable chromatographic artifacts such as column bleed.
- A selected subset of ions from a mass-defect analysis can be used to specify ion ranges for a 2D selected ion chromatogram. Mass-defect analyses expose patterns of ions according to their nominal mass and mass defect. Then, sub-patterns of interest, e.g., related to elemental composition and/or compound class, can be selected to specify ion ranges. Such ion ranges can be used to visualize the 2D separation of the associated compounds and/or to quantify them.

New software tools were designed and implemented in this research to support these operations. The supplement contains a discussion of important issues which are necessarily addressed by these tools. In particular, GC×GC–HRMS produces large data with many ion-peak centroids. The data size poses a challenge for visualization and other operations; and, the m/z variability among centroids for the same ion in different spectra poses a challenge for comprehensive analysis. The methods that were developed to address these challenges are described here.

Two alternative approaches were implemented in the software to combine centroids from multiple spectra by summing intensities and computing a single m/z value for centroids which vary over a small range. The operation also reduces the data size (e.g., for visualization) by combining centroids.

- Fixed-interval method. The first approach simply rounds the m/z values to reduce precision, then sums the intensities of centroids rounded to the same m/z. Within each rounding interval, the m/z for the summed intensity is computed as the weighted average (i.e., the sum of the products of the m/z values multiplied by the associated intensities and that sum divided by the sum of the intensities). Rounding to a resolution that is finer than provided by the instrument (as illustrated in Fig. S3, with interval 10^{-6} Da) results in intervals that are too small to collect all of the centroids for the same ion, so there are several summed centroids for the same ion. At the other extreme of too little resolution, rounding to the nearest integer would collect all of the centroids for each integer mass (from bottom-to-top along each nominal mass in Fig. S2), thereby sacrificing the high mass-resolution of the original data.
- Tent-pole clustering method. The second approach takes large intensity centroids as tent-poles for intervals within which intensities are summed and the m/z is computed as the weighted average of centroids in the interval around the tent-pole. The centroid with the largest intensity claims the maximum interval size allowed by the user. Then, centroids with progressively smaller intensities claim intervals up to the maximum size except where limited by intervals for centroids with larger intensities.

The advantages of the fixed-interval approach include simplicity and consistent, fixed-size intervals, but a draw-back is that the delineation between intervals is arbitrary and so centroids for the same ion may be divided into two adjacent intervals, even with appropriately sized intervals. The advantage of the tent-pole clustering approach is that it uses the data to more appropriately delineate intervals, but draw-backs include algorithmic sophistication and ad hoc, variable-sized intervals.

With both approaches, it is desirable to set a small interval size (either fixed or maximum tent-size) that will collect all of the centroids from the same ion despite their varying m/z values. Setting the interval size too small will place centroids from the same ion in multiple intervals, whereas setting the interval too large may sacrifice the mass precision available in the data by putting the centroids for different ions in the same interval.

Fig. 5 illustrates these tradeoffs by using the tent-pole clustering method with four different maximum intervals for the data shown in Fig. S3. In Fig. 5a, the maximum interval is ±0.001. As in Fig. S3, the two ions and their isotopes are discernable ($C_{12}H_6Br_4O^+$ across the top and $C_{12}H_4Br_4O^+$ across the bottom), but the centroids of each isotope are combined into many distinct intervals, which is undesirable. In Fig. 5b, the maximum interval is ±0.005 Da. In this plot, the largest isotopic ions are clearer because nearly all of the centroids for each isotopic ion are combined in single intervals. In Fig. 5c, the maximum interval is ±0.010 Da. In this plot, the combined centroids of each isotopic ion are even more clearly distinct. In Fig. 5d, the maximum interval is ±0.050 Da. In this plot, the centroids of the isotopes of the two different ions are combined due to the loss of resolution that is required to separate them. Of these plots, a maximum interval of ±0.010 Da (Fig. 5c) yields the best visual result, which is consistent with the approximate vertical distribution of centroids for each ion seen in Fig. 5a. As can be seen, the number, relative positions, and proportional areas of the circles in Fig. 5c for each of the isotopes of both ions are consistent with the expected isotopic distributions shown in Fig. S4 (although the mass scales are different, with m/z in Fig. S4 and −H/+Cl mass in Fig. 5).

Using the appropriate interval size to generate the combined mass spectrum from multiple mass spectra both reduces the size of the data, which facilitates visualization, and collects centroids from the same ion into a single centroid, which facilitates interpretation.

With GC×GC, mass-defect analysis can be used to generate 2D SICs to visualize the analyte peaks with specific masses and mass defects. Fig. 6 shows polygons drawn to select each of the two sets of isotopic ions using the mass-defect plot in Fig. 5c (tent-pole clustering with maximum interval ±0.010 Da). On the left, isotopic ions for $C_{12}H_6Br_4O^+$ are selected and, on the right, isotopic ions for $C_{12}H_4Br_4O^+$ are selected. For each selected centroid, a mass range is added to the SIC, with a user-defined tolerance. For example, if a centroid selected from the mass-defect analysis has m/z = 485.711 and the user-defined mass range is ±0.005 Da, then the selected ion range is 485.706–485.716. The combined mass range for the SIC is computed as the union of the ranges for all selected centroids. Note that the SIC m/z ranges are determined from the selected combined centroids, but the SIC ranges are applied to the original centroid data. Fig. 7 illustrates the SICs generated in this fashion (with ±0.005 Da tolerance) from the centroids selected in Fig. 6. Fig. 7a shows the SIC from the mass ranges for the selected $C_{12}H_6Br_4O^+$ isotopic ions, and Fig. 7b shows the SICs from the mass ranges for the selected $C_{12}H_4Br_4O^+$ isotopic ions. As can be seen in this example, 2D SICs generated from mass defect analysis can clearly differentiate compounds with different

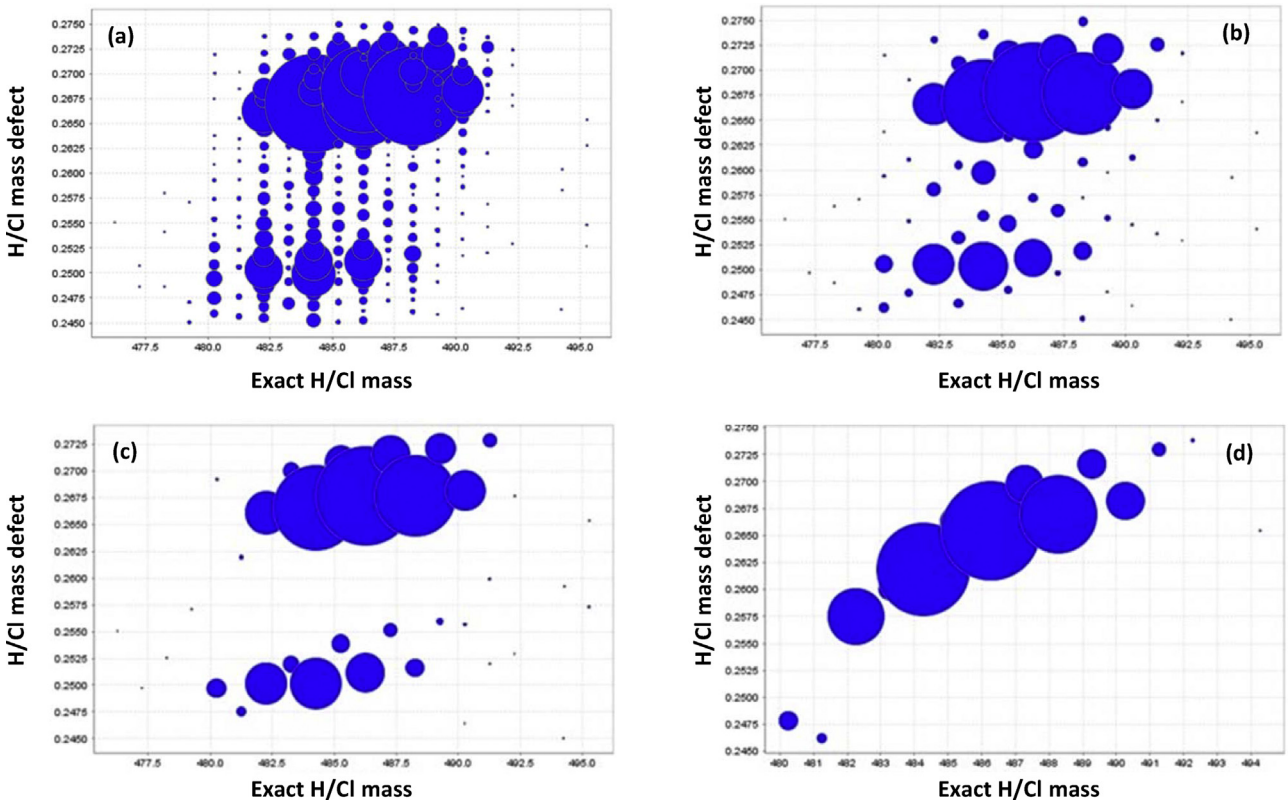

Fig. 5. A region of the Kendrick mass-defect plot shown in Fig. S2 with tent-pole centroid clustering with four different maximum-size intervals: (a) ±0.001 Da, (b) ±0.005 Da, (c) ±0.010 Da, and (d) ±0.050 Da.

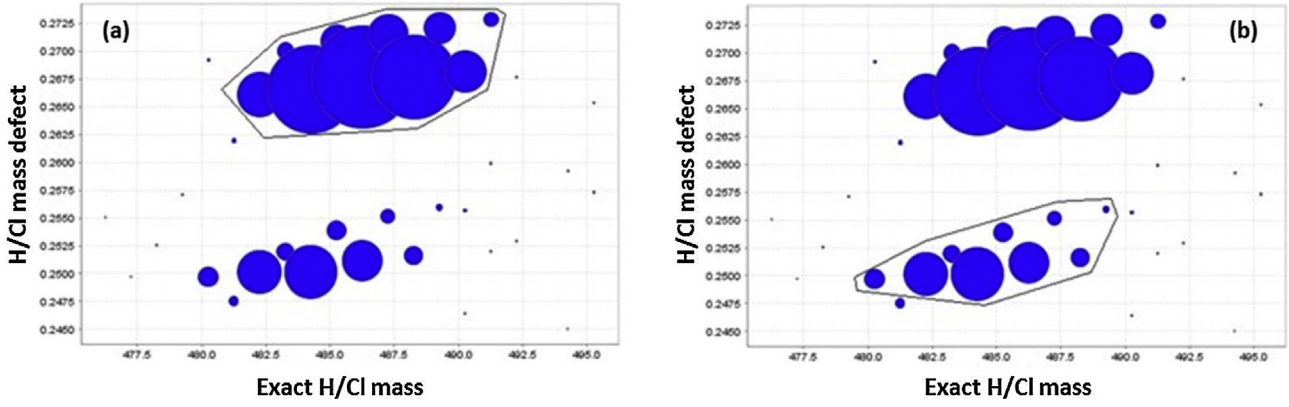

Fig. 6. Selection boxes outline the two sets of isotopic ions from Fig. 5c: (a) isotopic ions for $C_{12}H_6Br_4O^+$ and (b) isotopic ions for $C_{12}H_4Br_4O^+$.

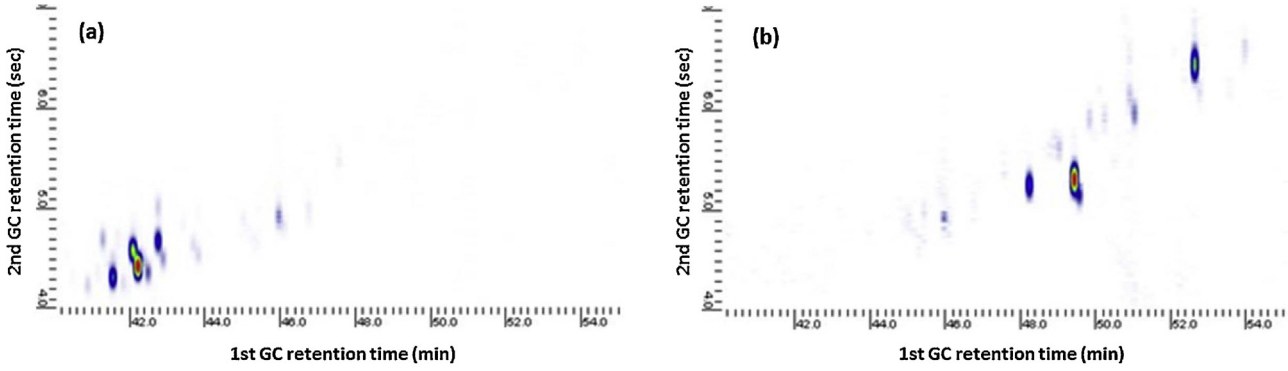

Fig. 7. The selected mass chromatograms for the isotopic ions selected in Fig. 6: (a) for $C_{12}H_6Br_4O^+$ and, (b) for $C_{12}H_4Br_4O^+$.

molecular characteristics. This is the approach used in the analysis of the electronic waste, presented in Section 2.1.

4. Conclusion

The research described in this paper utilizes mass defect analysis with GC×GC–HRMS systems. Chlorinated and brominated compounds can be easily filtered from complex data sets using −H/+Cl mass defect plot visualizations. Data from nontraditional Kendrick mass defect plots were used to make 2D SICs which provide significantly more information on the components of compound groups than 1D SICs. NIST library search results along with accurate mass measurement information from the data acquired in EI mode significantly aided in the assignment of chemical formula of the molecular and corresponding fragment ions. The ECNI measurements with GC×GC and Kendrick mass analysis produced similar results to the EI data for several compounds. However, some compounds showed abundant Cl^- and Br^- peaks instead of molecular ions. The ECNI method is especially good for quantitative analysis of low-concentration compounds in challenging samples. The combination of new methods GC×GC, HR-TOFMS, and the Kendrick mass defect visualization for the analysis of a complex samples is a very powerful and useful tool for detailed qualitative analysis, especially for unknown compounds.

Appendix A. Supplementary data

Supplementary data associated with this article can be found, in the online version, at http://dx.doi.org/10.1016/j.chroma.2015.03.050.

References

[1] L. Ramos, Comprehensive Analytical Chemistry, Elsevier, U.K., 2009.
[2] T. Ieda, N. Ochiai, T. Miyawaki, T. Ohura, Y. Horii, Environmental analysis of chlorinated and brominated polycyclic aromatic hydrocarbons by comprehensive two-dimensional gas chromatography coupled to high-resolution time-of-flight mass spectrometry, J. Chromatogr. A 1218 (21) (2011) 3224–3232, http://dx.doi.org/10.1016/j.chroma.2011.01.013.
[3] N. Ochiai, T. Ieda, K. Sasamoto, et al., Stir bar sorptive extraction and comprehensive two-dimensional gas chromatography coupled to high-resolution time-of-flight mass spectrometry for ultra-trace analysis of organochlorine pesticides in river water, J. Chromatogr. A 1218 (39) (2011) 6851–6860, http://dx.doi.org/10.1016/j.chroma.2011.08.027.
[4] S. Hashimoto, Y. Takazawa, A. Fushimi, et al., Global and selective detection of organohalogens in environmental samples by comprehensive two-dimensional gas chromatography-tandem mass spectrometry and high-resolution time-of-flight mass spectrometry, J. Chromatogr. A 1218 (24) (2011) 3799–3810, http://dx.doi.org/10.1016/j.chroma.2011.04.042.
[5] S. Hashimoto, Y. Zushi, A. Fushimi, Y. Takazawa, K. Tanabe, Y. Shibata, Selective extraction of halogenated compounds from data measured by comprehensive multidimensional gas chromatography/high resolution time-of-flight mass spectrometry for non-target analysis of environmental and biological samples, J. Chromatogr. A 1282 (October) (2013) 183–189, http://dx.doi.org/10.1016/j.chroma.2013.01.052.
[6] Y. Zushi, S. Hashimoto, A. Fushimi, Y. Takazawa, K. Tanabe, Y. Shibata, Rapid automatic identification and quantification of compounds in complex matrices using comprehensive two-dimensional gas chromatography coupled to high resolution time-of-flight mass spectrometry with a peak sentinel tool, Anal. Chim. Acta 778 (2013) 54–62, http://dx.doi.org/10.1016/j.aca.2013.03.049.
[7] F.W. McLafferty, F. Turecek, Interpretation of Mass Spectra, 4th edition, University Science Books, Sausalito, California, 1993.
[8] D.C. Hilton, R.S. Jones, A. Sjodin, A method for rapid, non-targeted screening for environmental contaminants in household dust, J. Chromatogr. A 1217 (2010) 6851–6856, http://dx.doi.org/10.1016/j.chroma.2010.08.039.
[9] E. Hoh, N.G. Dodder, S.J. Lehotay, K.C. Pangallo, C.M. Reddy, K.A. Maruya, Nontargeted comprehensive two-dimensional gas chromatography/time-of-flight mass spectrometry method and software for inventorying persistent and bioaccumulative contaminants in marine environments, Environ. Sci. Technol. 46 (2012) 8001–8008.
[10] M. Pena-Abaurrea, K.J. Jobst, R. Ruffolo, L. Shen, R. McCrindle, P.A. Helm, E.J. Reiner, Identification of potential novel bioaccumulative and persistent chemicals in sediments from Ontario (Canada) using scripting approaches with GC×GC-TOF MS analysis, Environ. Sci. Technol. 48 (16) (2014) 9591–9599, http://dx.doi.org/10.1020/es5018152.
[11] D.C. Muir, P.H. Howard, Are there other persistent organic pollutants? A challenge for environmental chemists, Environ. Sci. Technol. 40 (23) (2006) 7157–7166.
[12] M. Scheringer, S. Strempel, S. Hukari, C.A. Ng, M. Blepp, K. Hungerbuhler, How many persistent organic pollutants should we expect? Atmos. Pollut. Res. 3 (2012) 383–391.
[13] Edward Kendrick, A mass scale based on CH2 = 14.000 for high resolution mass spectrometry of organic compounds, Anal. Chem. 35 (1963) 2146–2154.
[14] C.a. Hughey, C.L. Hendrickson, R.P. Rodgers, a.G. Marshall, K. Qian, Kendrick mass defect spectrum: a compact visual analysis for ultrahigh-resolution broadband mass spectra, Anal. Chem. 73 (19) (2001) 4676–4681.
[15] L. Sleno, The use of mass defect in modern mass spectrometry, J. Mass Spectrom. 47 (2) (2012) 226–236, http://dx.doi.org/10.1002/jms.2953.
[16] V.Y. Taguchi, R.J. Nieckarz, R.E. Clement, S. Krolik, R. Williams, Dioxin analysis by gas chromatography-Fourier transform ion cyclotron resonance mass spectrometry (GC-FTICRMS), J. Am. Soc. Mass Spectrom. 21 (11) (2010) 1918–1921, http://dx.doi.org/10.1016/j.jasms.2010.07.010.
[17] K.J. Jobst, Li Shen, E.J. Reiner, V.Y. Taguchi, P.A. Helm, R. McCrindle, S. Backus, The use of mass defect plots for the identification of (novel) halogenated contaminants in the environment, Anal. Bioanal. Chem. 405 (2013) 3289–3297.
[18] S. Fernando, K.J. Jobst, V.Y. Taguchi, P.A. Helm, E.J. Reiner, B.E. McCarry, Identification of the halogenated compounds resulting from the 1997 Plastimet Inc. Fire in Hamilton, Ontario, using comprehensive two-dimensional chromatography and (Ultra)high-resolution mass spectrometry, Environ. Sci. Technol. 48 (18) (2014) 10656–10663.
[19] A.L. Myers, K.J. Jobst, S.A. Mabury, E.J. Reiner, Using mass defect plots as a discovery tool to identify novel fluoropolymer thermal decomposition products, J. Mass Spectrom. 49 (4) (2014) 291–296.
[20] N. Ali, S. Harrad, E. Goosey, H. Neels, A. Covaci, Novel brominated flame retardants in Belgian and UK indoor dust: implications for human exposure, Chemosphere 83 (10) (2011) 1360–1365.
[21] P.I. Johnson, H.M. Stapleton, A. Sjodin, J.D. Meeker, Relationships between polybrominated diphenyl ether concentrations in house dust and serum, Environ. Sci. Technol. 44 (14) (2010) 5627–5632.
[22] E. Sverko, G.T. Tomy, E.J. Reiner, Y.-F. Li, B.E. McCarry, J.A. Arnot, R.J. Law, R.A. Hites, Dechlorane Plus and related compounds in the environment: a review, Environ. Sci. Technol. 45 (12) (2011) 5088–5098.